Structural optimizing of fiber-reinforced composite dentures using stress-induced material transformation

YungChung Chen*[1] and Alex Fok[2]

1. **Institute Of Oral Medicine, College Of Medicine, National Cheng Kung University**
2. **Minnesota Dental Research Center for Biomaterials and Biomechanics, School of Dentistry, University of Minnesota, Minneapolis, MN**

***Corresponding author: chen1954@umn.edu**

ABSTRACT

Because of their minimal invasion and low cost, fiber-reinforced composite fixed partial dentures (FRCFPD) have become an attractive option for single tooth replacement. However, denture failure can result from inappropriate layouts of the constituent materials. A stress-induced material transformation (SMT) technique is applied here to seek optimal material arrangements for the bridge and cantilever FRCFPD. Structural optimization is performed using ABAQUS via a user subroutine which iteratively reinforces regions with high stresses with stronger fiber materials. The fibers introduced are closely aligned with the maximum principal stress in all locations. Compared to the conventional designs, the peak tensile stress is reduced by ~30% and ~45% for the bridge and cantilever FRCFPD, respectively. Furthermore, the resulting cavity design reduces the peak tensile stress at the tooth-denture interface by ~70%. Validation tests demonstrate a much lower level of micro-cracking and smoother load-displacement behavior, i.e. higher fracture resistance, in the optimized designs.

Keywords: Structural optimization, finite element, stress-induced material transformation and fiber-reinforced composite

Introduction

The breakthrough in the strength of dental adhesive material has brought more flexibility to the design of dental prosthesis, such as the concept of minimally invasive dentistry. The treatment philosophy of minimally invasive dentistry is to reduce unnecessary tooth preparation and to preserve healthy tooth tissue as much as possible (Murdoch-Kinch and McLean 2003). But conventional meal-ceramic or all-ceramic restoration does not conform to this principle, because they usually require larger amount of tooth reduction to ensure adequate thickness for mimicking the neighboring teeth (Rosenstiel, Land et al. 2006). Therefore, fiber-reinforced composite (FRC) system, which can provide excellent tooth-colored appearance and allow minimizing the amount of tooth removal, starts to be widely applied in minimally invasive dentistry.

Clinically, the ideal indication of FRC restoration is single tooth replacement. Depending on the periodontal status of the abutment tooth, the position of the missing tooth, individual's occlusal force or any existing parafunctional habits, the option of the restoration design can be conventional dental bridges, supported by two abutments at both ends of the edentulous area or cantilevered dental bridges, supported on only one end (Freilich 2000). In addition, the retainer design is not restricted to a full-coverage crown only; an inlay-retained design which can further decrease the amount of unnecessary tooth reduction is also available. However, the mean survival rate of FRCFPD, reported at 2009 in a systemic review (Heumen, Kreulen et al. 2009), was only 73.4% at 4.5 years. Two major failure modes were reported as debonding at tooth/retainer interface and structural fracture, which can occur at the loading point (Song, Yi et al. 2003; Dyer, Lassila et al. 2005; Ozcan, Breuklander et al. 2005), the pontic and the connectors linking the retainer and the pontic (Vallittu 1998; Kolbeck, Rosentritt et al. 2002; Li, Swain et al. 2004). In comparison with the conventional metal-ceramic FPD, the durability of FRCFPD needs to be improved.

Several studies have shown that the main contributing factor of clinical failure is inadquate fiber orientation and position (Magne, Perakis et al. 2002; Nakamura, Ohyama et al. 2005; Rappelli, Scalise et al. 2005; Ootaki, Shin-Ya et al. 2007). In order to elongate the lifespan of FRCFPD, many researchers tried to discover the optimal fiber position and orientation. In earlier days, conventional compression test have been the primary approach for comparing the mechanical performance among various designs (Chung, Lin et al. 1998; Ellakwa, Shortall et al. 2001; Dyer, Lassila et al. 2004; Dyer, Lassila et al. 2005; Narva, Lassila et al. 2005). However, this approach requires huge amount of material expense and time investment for specimen fabrication. Furthermore, the influence of changing material layout on the stress distribution in the structure can not be visualized. Thus, finite element (FE) analysis has been introduced to guide the designing process of FRCFPD (Li, Swain et al. 2005; Keulemans, De Jager et al. 2008; Shinya, Yokoyama et al. 2008; Shinya, Lassila et al. 2009).

Although FE analysis can help researchers compare structural stress distributions among different designs, one often needs to modify the design and analyze the results repeatedly before arriving at a satisfactory solution. This “trial-and-error” process is very time-consuming and it is often not possible to confirm if the final design is really optimal. To accelerate the design process, modern structural optimization techniques, which are widely used in designing engineering components and structures, can be used to design dental implants and bridges.

Several structural optimization techniques have been applied in industrial design, including Computer Aided Optimization (CAO) and the Soft Killed Option (SKO) developed at the Karlsruhe Research Center (Mattheck 1998), Bi-directional Evolutionary Structural Optimization (BESO) (Xie and Steven 1993), the Variable Thickness Sheet model (Rossow 1973), and the SHAPE method (Atrek 1992). Amongst these, techniques inspired by the adaptive growth of biological structures have proved to be very effective in producing structures that are optimal in terms of stress distribution.

In the present project, the authors applied the stress-induced material transformation (SMT) technique, in which the material property of each element can be changed according to the local stress, in the designing process of FRCFPD. The aim of this study was to obtain the optimal fiber layout of two common types of inlay-retained FRCFPD, the 3-unit conventional and the 2-unit cantilever bridge. Furthermore, the clinical performance of the optimized design was also in vitro validated.

Materials and Methods

1. *Shape optimization of FRCFPD design using SMT technique*

The shape optimization of 3-unit inlay-retained FRCFPD was done by Dr. Shi Li and the detailed procedures and results can be referred to (Shi and Fok 2009). Only the details for optimizing 2-unit cantilevered FRCFPD were described here. Especially for cantilever design, one should first consider lowering the interfacial tensile stress to reduce the risk of debonding. To achieve that, the authors applied a two-steps approach for the shape optimization of the 2-unit inlay-retained cantilever bridge in this study.

1.1 FE model construction

A human mandibular first molar was embedded in the orthodontic resin to form a physical model. Then a second premolar pontic was fabricated using composite resin (Filtek Z250 universal composite, 3M ESPE, USA) and attached to the mesial surface of the molar (Figure 1).

Figure 1 The physical model of mandibular first molar and second premolar pontic

The whole entity was scanned using micro-CT scanner (HMX-XT 255, X-tek system, United Kingdom) with a tube voltage of 100 Kv and a tube current of 170 µA. A total of 720 projection and four frames per projection was taken. The acquired images were reconstructed into 3D volume using the software CT Pro 3D (Nikon Metrology, Brighton, MI, USA). The segmentation process of the 3D volume was manipulated in the software Avizo 6.0 (Visualization Sciences Group, Burlington, MA, USA) to partition each material such as enamel, dentin, bone and composite resin. The 3D surface for each component was created and then exported as a stereolithography (STL) file. The STL file was imported into the software Hypermesh 10.0 (HyperWorks, Altair Engineering, Troy, MI, USA) for finite element model construction.

Because the present study mainly focused on stress distributions of the restoration and tooth structures, the realistic morphology of mandibular jaw bone was not modeled. A rectangular block of 11 mm thick with a top layer of 2 mm thick which represent the cancellous and cortical bone respectively was used to simulate the surrounding bone tissues (Figure 2). In addition, the mesh density of the restoration and tooth structure was much finer than others in the bone block. All the interfaces were assumed to be tied perfectly in the FE model. The material property for each component was listed in Table 1. A concentrated force of 200 N was loaded on the mesial fossa of the premolar pontic to simulate the worst chewing scenario. The boundary condition was defined that all displacements was fixed at the bottom of the bone structure.

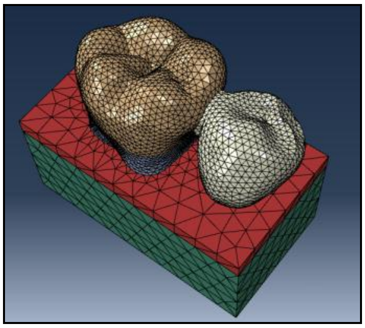

Figure 2 The FE model of 2-unit cantilever bridge

Table 1 Material properties used in the FE model

Material	**Elastic Modulus (GPa)**		**Poisson ratio**	**Ref.**
Enamel	84.1		0.33	1
Dentin	18.6		0.31	2
Cortical Bone	13.7		0.3	3
Cancellous Bone	1.37		0.3	3
Composite	14		0.31	4
Glass Fiber	Ex 37	Vxy 0.27	Gxy 3.1	5
	Ey 9.5	Vxz 0.34	Gxz 3.5	
	Ez 9.5	Vyz 0.27	Gyz 3.1	

1.2 Two-steps shape optimization

Shape optimization was carried out using the software ABAQUS 6.10-EF1 (Dassault Systèmes Simulia, Waltham, MA, USA) in conjunction with a user-defined material subroutine, which defined the constitutive model and mechanical behavior of a material according to its stress state. The first step of shape optimization was to obtain the optimal cavity preparation by applying the subroutine within the tooth tissues only. Then the subroutine was applied within the restoration with the optimized retainer design to seek optimal fiber layout.

In the first step, the material session of the enamel and dentin was defined as User-Material in the input file so that it would call the SMT subroutine to update their solution-dependent material properties during the stress analysis. Initially, the material properties of enamel and dentin were set the same as those in the Table 1 and stress analysis was performed to obtain stress distribution of the original material layout. Subsequently, the material properties of the User-Material session were modified according to the local stresses. To reduce the interfacial stress, all elements with the local stresses larger than the assumed failure stress were gradually replaced with “softer” composite resin material. All other parameters, including material properties for the teeth and bones outside the User-Material session, the applied load and boundary conditions, were kept the same during the whole analysis.

In the second step, an inlay retainer was created within the tooth structure using the cavity design guided in the previous step. The material properties of enamel and dentin were reverted to those in the Table 1 and the material session of the restoration was defined as User-Material. To obtain the proper reinforcing layout within the restoration, all elements with the local stresses larger than the assumed failure stress were gradually replaced with “stronger” fiber material. All the material transformation process would continue iteratively until the results converged. The selection of the failure stress was based on the bonding strength of resin material for the first step and fracture strength of resin material for the second step.

1.3 Final comparison between the conventional and optimal design

A step-box shaped retainer was used for the model of the conventional design of 2-unit cantilever FRCFPD (Keulemans, De Jager et al. 2008; Bortolotto, Monaco et al. 2010). The width of the box started as 2.5 mm in the mesial fossa and was projected to 3.5 mm on the marginal ridge. The depth of the occlusal inlay was 2 mm and the occlusal step was 4 mm. The glass fiber was horizontally placed and fully embedded with composite resin in the middle third of the connector region and the mesial part of the pontic (Figure 3). The design provided by the optimization exercise sometimes contains features that may not be able to be realized in practice. To construct the model for the final comparison, practical issues, such as the actual cavity shape that can be made, were also taken into account. Therefore, a simplified FE model based on the optimized substructural design constructed and compared with the conventional design.

Finally, stress analyses of the shape-optimized and conventional designs were carried out to compare their mechanical performances. The local stresses at the interface of tooth and restoration and within the restoration were compared between the two designs.

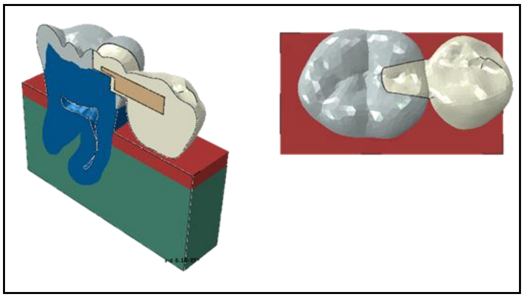

Figure 3 The conventional design of 2-unit cantilevered FRC bridge

2 In vitro validation for 3-unit optimized FRCFPD

The detailed procedures of in vitro validation have been published (Chen, Li et al. 2011). A brief summary was given as follows: mandibular first molar and first premolar was selected and mounted in PMMA resin to reproduce the same edentulous condition as that of the FE model (Shi and Fok 2009). The optimized and conventional material layouts of the dental restoration were prepared. Each individual specimen was tested with compressive load up to 400 N using a servo-hydraulic testing machine. During loading, both the force and displacement of the loading sphere were recorded. Furthermore, to synchronously and nondestructively monitor the occurrence of micro-cracking, a two-channel acoustic emission measurement system (AE) was used during mechanical test.

After mechanical loading, all specimens were examined using optical a stereo-microscope to look for surface cracking and chipping. Micro-CT scan was also performed to detect subsurface cracks. The load-displacement data and the AE results obtained from the compressive test were processed using the software Matlab R2009b (Mathworks, Natick, MA, USA). To correlate the AE signals with the load drops in the load-displacement curve, the plot of AE signal amplitudes versus time was superimposed upon the load-displacement curve. The accumulated number of all AE events and the amplitude of individual AE event for each specimen were extracted. The sum of amplitudes from all AE events was then calculated to provide a measure of the total strain energy released by each specimen.

Results

1 Shape optimization of 2-unit cantilevered FRC bridge

Assuming different level of the bonding strength as the failure stress (σ_{Ref}), all the retainer designs derived from the SMT optimization were shoveled-shaped (Figure 4). Results from the SMT optimization also indicate that larger amount of cavity preparation was required if lower bonding strength was considered. A failure stress of 25 MPa, which is lower than the clinical reported bonding strength, was used for the model construction of the optimal design and the subsequent model comparison. The size of the retainer was slightly smaller than the conventional step-box shaped design (26.122 mm^3 versus 26.226 mm^3). However, in terms of the area of the bonding surface, the optimal design was 17.5% smaller than the conventional one (31.314 mm^2 versus 37.980 mm^2).

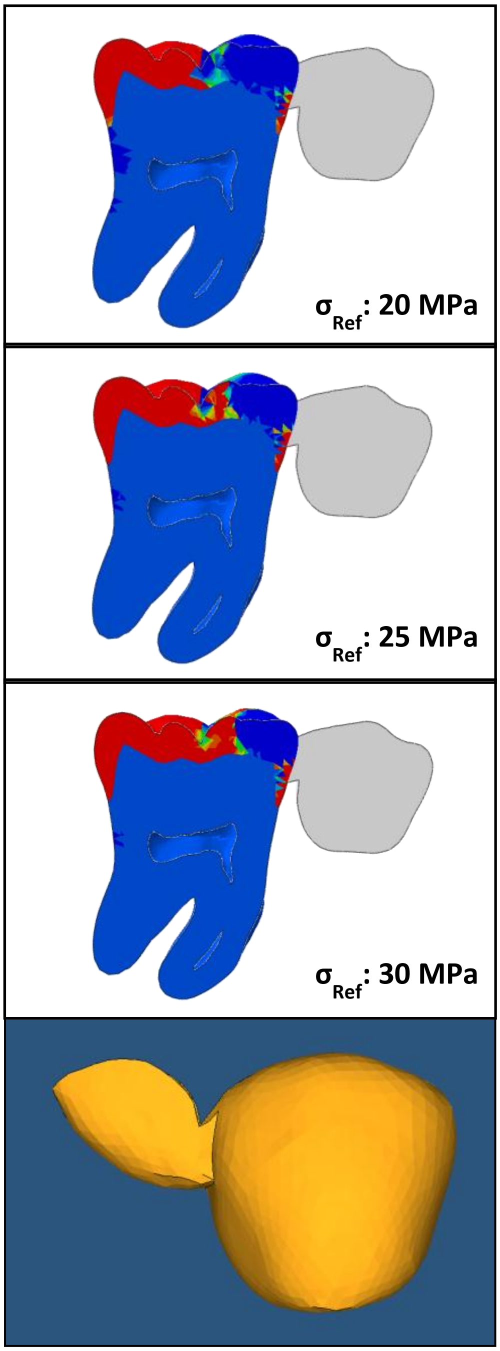

Figure 4 The results from the first step of SMT optimization

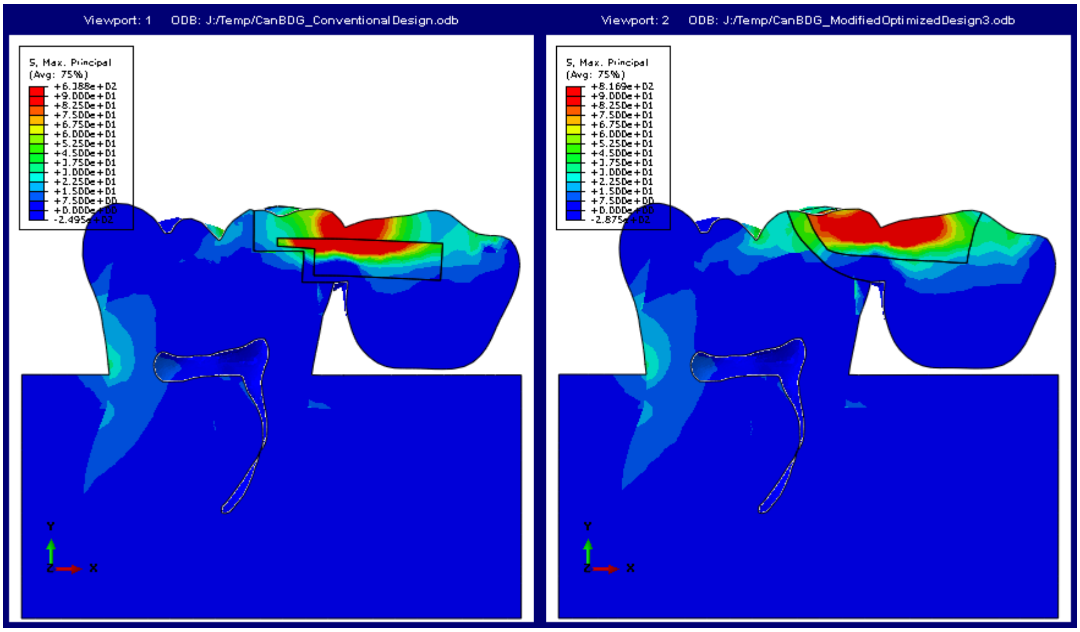

Figure 5 Stress profiles of two designs

According to the results from the SMT optimization, fibers should be placed at the top of the connector region where tensile stress was high. Figure 5 showed the stress profiles of the two designs. High tensile stresses can be seen on the occlusal third of the connector region. In the optimal design, the fiber substructure carries most of high tensile stresses. However, the conventional design was not reinforced properly. Stress concentration was only found on the top of the fiber substructure and high tensile stress still can be found in the veneering composite. Incontinuous stress profile can also be found at the interface between the fiber and the veneering resin which would result in the fiber delamination.

Compared with the conventional design, the shovel-shaped cavity preparation has ~70% reduction (189.6 MPa versus 57.04 MPa) in interfacial tensile stress (Figure 6a). With the optimized design, the maximum principal stress in the veneering composite was also reduced by ~45% (638.8 MPa versus 356.5 MPa; Figure 6b).

2 In vitro validation

A brief summary about the in-vitro validation of 3-unit inlay-retained bridge was provided here. Further details can be referred to (Chen, Li et al. 2011). Twenty specimens with the conventional design were fractured but only six specimens from the optimized group were found with small cracks under the connector area. Micro-CT scan also indicated that the maximum crack length of the optimized design was far shorter than the conventional design (0.07 mm versus 3.72 mm). Smoother and steeper load-displacement curves, which indicated stiffer and stronger in resisting the fractures, can also be observed in the optimized group.

Table 2 showed the results of the AE measurement (Chen, Li et al. 2011). Significantly higher mean number of AE events per specimen was noticed in the group of the conventional design (conventional group: 2969 ± 1034; optimized group: 38 ± 42; P-value < 0.001). No statistically significant difference was found between the two groups in the mean amplitude for each AE event, there was (conventional group: 45.4 ± 0.5 dB; optimized group: 44.4 ± 10.7 dB; P-value = 0.65). The mean accumulated amplitude of all AE events per specimen, a measure of the strain energy released calculated by multiplying together the mean amplitude of the AE signal and the mean number of AE events, further demonstrated the significant difference in the mechanical performance between the two groups of specimens (conventional group: 134914.2 ± 47302.1 dB; optimized group: 1749.9 ± 1911.9 dB; P-value < 0.001).

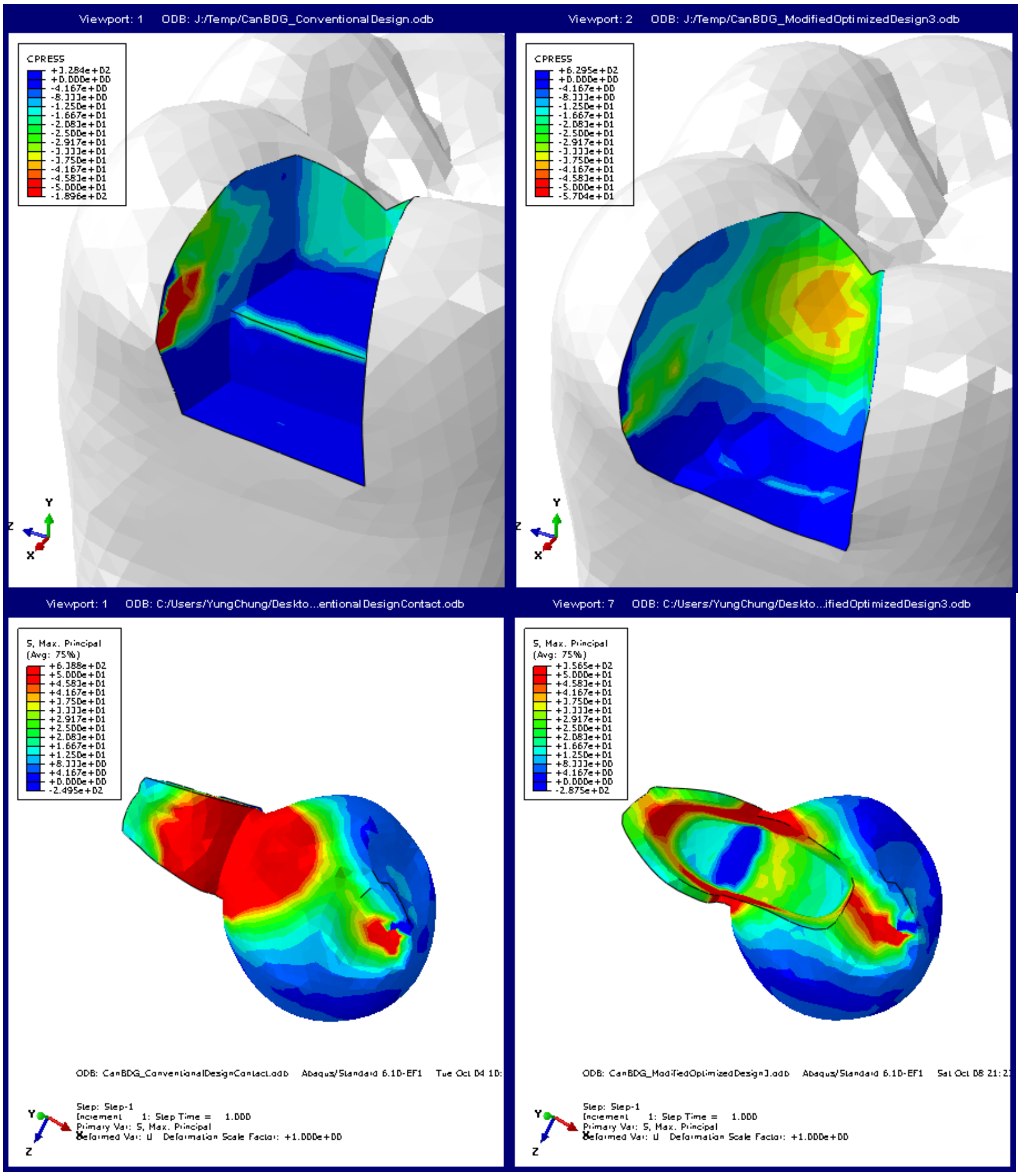

Figure 6 a: Interfacial stress comparison of two designs b: The stress distribution of two designs in the veneering composite

Discussion and Conclusion

The results of the 3-unit inlay-retained FRC bridge's shape optimization and in vitro validation indicated that the optimized design used the same amount of the reinforcing fiber as the conventional design but its mechanical performance was far better than the conventional design. Comparing the stress profiles between two designs, the material layout of the optimized design also aligned with the maximum principal stress trajectories.

Then, a more conservative but more challenging design, 2-unit cantilever bridge, was investigated using the SMT technique. Clinically, this type of restoration has been mainly used as an interim prosthesis. Also, most of studies mainly focused on the application of the cantilever bridge in the anterior region (Culy and Tyas 1998; Auplish and Darbar 2000). However, comparing with conventional 3-unit bridges, less damage to the healthy tooth tissue and easier to maintain oral hygiene have been the advantages for considering the use of such a dental prosthesis design.

As suggested by the SMT subroutine, the fiber has to be placed at the top of the connector. In this manner, high tensile stress can be mostly carried by the fiber material so that the maximum principal stress in the veneering composite can be also reduced by ~45%. In this study, the failure stress was selected as 25 MPa for optimizing the cavity design. This is because the authors would like to have similar cavity size between two designs so that the influence of changing the fiber layout can be reasonably compared. The bonding strength between the tooth and composite resin is usually higher than 25 MPa. Therefore, the size of the cavity preparation can be even smaller so that more tooth tissues can be preserved. Although the area of the bonding surface was reduced by 17.5 %, it is believed that lower interfacial stress would help restoration maintain its retention.

With its lower interfacial and structural stresses, the new, optimized design is expected to perform better mechanically than the conventional design. An in vitro study has been planned for its validation.

Table 2 Summary of AE measurements

Group	**The mean number of AE events (±SD)**	**The mean amplitude of AE signal (±SD) (dB)**	**Mean accumulated amplitude of all AE events (±SD) (dB)**
Conventional	2968.8 (±1033.5)	45.4 (±0.5)	134914.2 (±47302.1)
Optimized	37.7 (±41.6)	44.4 (±10.7)	1749.9 (±1911.9)
***P*-Value**	<0.001	0.65	<0.001

Reference

Atrek, E. (1992). SHAPE: a program for shape optimization of continuum structures. roc. 1st Int. Conf.: OPTI '89,. H. S. Brebbia C.A. . Southampton, U.K.: 135-144.

Auplish, G. and U. R. Darbar (2000). "Immediate anterior tooth replacement using fibre-reinforced composite." Dental update 27(6): 267-270.

Bortolotto, T., C. Monaco, et al. (2010). "In Vitro Assessment of Single-Retainer Tooth-Colored Adhesively Fixed Partial Dentures for Posterior Teeth." International Journal of Dentistry 2010.

Chen, Y., H. Li, et al. (2011). "In vitro validation of a shape-optimized fiber-reinforced dental bridge." Dental Materials 27(12): 1229-1237.

Chung, Lin, et al. (1998). "Flexural strength of a provisional resin material with fibre addition." Journal of Oral Rehabilitation 25(3): 214-217.

Culy, G. and M. J. Tyas (1998). "Direct resin-bonded, fibre-reinforced anterior bridges: A clinical report." Australian Dental Journal 43(1): 1-4.

Dyer, S. R., L. V. J. Lassila, et al. (2005). "Static strength of molar region direct technique glass fibre-reinforced composite fixed partial dentures." Journal of Oral Rehabilitation 32(5): 351-357.

Dyer, S. R., L. V. J. Lassila, et al. (2004). "Effect of fiber position and orientation on fracture load of fiber-reinforced composite." Dental Materials 20(10): 947-955.

Dyer, S. R., L. V. J. Lassila, et al. (2005). "Effect of cross-sectional design on the modulus of elasticity and toughness of fiber-reinforced composite materials." The Journal of Prosthetic Dentistry 94(3): 219-226.

Ellakwa, A. E., A. C. Shortall, et al. (2001). "The influence of fibre placement and position on the efficiency of reinforcement of fibre reinforced composite bridgework." Journal of Oral Rehabilitation 28(8): 785-791.

Freilich, M. A. (2000). Fiber-reinforced composites in clinical dentistry, Quintessence Pub. Co.

Heumen, C. C. M. v., C. M. Kreulen, et al. (2009). "Clinical studies of fiber-reinforced resin-bonded fixed partial dentures: a systematic review." European Journal of Oral Sciences 117(1): 1-6.

Keulemans, F., N. De Jager, et al. (2008). "Influence of retainer design on two-unit cantilever resin-bonded glass fiber reinforced composite fixed dental prostheses: an in vitro and finite element analysis study." The journal of adhesive dentistry 10(5): 355.

Kolbeck, C., M. Rosentritt, et al. (2002). "In vitro examination of the fracture strength of 3 different fiber-reinforced composite and 1 all-ceramic posterior inlay fixed partial denture systems." Journal of Prosthodontics 11(4): 248-253.

Li, W., M. V. Swain, et al. (2004). "Fibre reinforced composite dental bridge.: Part I: experimental investigation." Biomaterials 25(20): 4987-4993.

Li, W., M. V. Swain, et al. (2005). "Towards automated 3D finite element modeling of direct fiber reinforced composite dental bridge." Journal of Biomedical Materials Research Part B: Applied Biomaterials 74B(1): 520-528.

Magne, P., N. Perakis, et al. (2002). "Stress distribution of inlay-anchored adhesive fixed partial dentures: A finite element analysis of the influence of restorative materials and abutment preparation design." The Journal of Prosthetic Dentistry 87(5): 516-528.

Mattheck, C. (1998). Design in Nature, Springer.

Murdoch-Kinch, C. A. and M. E. McLean (2003). "Minimally invasive dentistry." The Journal of the American Dental Association 134(1): 87-95.

Nakamura, T., T. Ohyama, et al. (2005). "Finite element analysis of fiber-reinforced fixed partial dentures." Dental materials journal 24(2): 275.

Narva, K. K., L. V. J. Lassila, et al. (2005). "Flexural fatigue of denture base polymer with fiber-reinforced composite reinforcement." Composites Part A: Applied Science and Manufacturing 36(9): 1275-1281.

Ootaki, M., A. Shin-Ya, et al. (2007). "Optimum design for fixed partial dentures made of hybrid resin with glass fiber reinforcement by finite element analysis: effect of vertical reinforced thickness on fiber frame." Dental materials journal 26(2): 280-289.

Ozcan, M., M. H. Breuklander, et al. (2005). "The effect of box preparation on the strength of glass fiber-reinforced composite inlay-retained fixed partial dentures." The Journal of Prosthetic Dentistry 93(4): 337-345.

Rappelli, G., L. Scalise, et al. (2005). "Stress distribution in fiber-reinforced composite inlay fixed partial dentures." The Journal of Prosthetic Dentistry 93(5): 425-432.

Rosenstiel, S. F., M. F. Land, et al. (2006). Contemporary fixed prosthodontics. St. Louis, Mo., Mosby/Elsevier.

Rossow, M. P. (1973). "A finite element method for the optimal design of variable thickness sheets." AIAA journal 11: 1566.

Shi, L. and A. S. Fok (2009). "Structural optimization of the fibre-reinforced composite substructure in a three-unit dental bridge." Dent Mater 25(6): 791-801.

Shinya, A., L. Lassila, et al. (2009). "Three-dimensional finite element analysis of posterior fiber reinforced composite fixed partial denture: framework design for pontic." The European journal of prosthodontics and restorative dentistry 17(2): 78.

Shinya, A., D. Yokoyama, et al. (2008). "Three-dimensional finite element analysis of metal and FRC adhesive fixed dental prostheses." The journal of adhesive dentistry 10(5): 365.

Song, H.-Y., Y.-J. Yi, et al. (2003). "Effects of two preparation designs and pontic distance on bending and fracture strength of fiber-reinforced composite inlay fixed partial dentures." The Journal of Prosthetic Dentistry 90(4): 347-353.

Vallittu, P. K. (1998). "The effect of glass fiber reinforcement on the fracture resistance of a provisional fixed partial denture." The Journal of Prosthetic Dentistry 79(2): 125-130.

Xie, Y. M. and G. P. Steven (1993). "A simple evolutionary procedure for structural optimization." Computers & Structures 49(5): 885-896.